The Journal of Chemical Physics

RESEARCH ARTICLE | NOVEMBER 22 2023

Tuning perovskite nanocrystal superlattices for superradiance in the presence of disorder

Special Collection: 2023 JCP Emerging Investigators Special Collection

T. P. Tan Nguyen ; Liang Z. Tan ; Dmitry Baranov

J. Chem. Phys. 159, 204703 (2023)
https://doi.org/10.1063/5.0167542
CHORUS

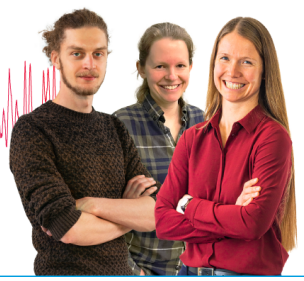

AIP Publishing

The Journal of Chemical Physics ARTICLE pubs.aip.org/aip/jcp

Tuning perovskite nanocrystal superlattices for superradiance in the presence of disorder

Cite as: J. Chem. Phys. 159, 204703 (2023); doi: 10.1063/5.0167542
Submitted: 13 July 2023 • Accepted: 15 September 2023 •
Published Online: 22 November 2023 • Corrected: 8 December 2023

T. P. Tan Nguyen,[1,a] Liang Z. Tan,[2] and Dmitry Baranov[3,a]

AFFILIATIONS

[1] M2I Formation, Sophia Antipolis, Mougins 06250, France
[2] Molecular Foundry, Lawrence Berkeley National Laboratory, Berkeley, California 94720, USA
[3] Division of Chemical Physics, Department of Chemistry, Lund University, P.O. Box, 124, SE-221 00 Lund, Sweden

Note: This paper is part of the 2023 JCP Emerging Investigators Special Collection.
[a] **Authors to whom correspondence should be addressed:** phuctan3108@gmail.com and dmitry.baranov@chemphys.lu.se

ABSTRACT

The cooperative emission of interacting nanocrystals is an exciting topic fueled by recent reports of superfluorescence and superradiance in assemblies of perovskite nanocubes. Several studies estimated that coherent coupling is localized to a small fraction of nanocrystals (10^{-7}–10^{-3}) within the assembly, raising questions about the origins of localization and ways to overcome it. In this work, we examine single-excitation superradiance by calculating radiative decays and the distribution of superradiant wave function in two-dimensional $CsPbBr_3$ nanocube superlattices. The calculations reveal that the energy disorder caused by size distribution and large interparticle separations reduces radiative coupling and leads to the excitation localization, with the energy disorder being the dominant factor. The single-excitation model clearly predicts that, in the pursuit of cooperative effects, having identical nanocubes in the superlattice is more important than achieving a perfect spatial order. The monolayers of large $CsPbBr_3$ nanocubes (L_{NC} = 10–20 nm) are proposed as model systems for experimental tests of superradiance under conditions of non-negligible size dispersion, while small nanocubes (L_{NC} = 5–10 nm) are preferred for realizing the Dicke state under ideal conditions.

I. INTRODUCTION

The optical properties of self-assembled colloidal nanocrystals are of fundamental and practical interest. The reports of superfluorescence[1–6] and superradiance[7–9] in ordered assemblies (superlattices) of perovskite nanocrystals are recent examples of collective optical effects. Combining such phenomena with scalable self-assembly[10] may lead to the low-cost fabrication of miniature coherent light sources for photonics and optical information processing. These systems form a rich playground where the material properties of constituent nanocrystals and the superstructure could be designed to control the cooperative light emission.

The idealized cooperative light emission (e.g., superradiance[11] and superfluorescence[12]) relies on identical emitters that are coupled via the electromagnetic field and form a Dicke ladder of macroscopic states. Molecular and atomic gases have been historically used as experimental systems that can approach such ideal conditions.[13,14] Semiconductor nanocrystals, resembling "artificial atoms," are interesting as quantum emitters with facile tunability of emission frequency by changing nanocrystals' size or composition. Nonetheless, their assemblies feature numerous inhomogeneities. For example, a realistic batch of colloidal nanocrystals is characterized by a distribution of sizes, shapes, and different surface passivations.[15] A nanocrystal superlattice also contains further imperfections such as vacancies,[16] variation in the superlattice periodicity,[17] and strain.[18] These experimental realities make nanocrystal emitters distinguishable from each other and introduce energy disorder to the system.

The imperfections pose a general question of how the energetic and spatial disorder influence the macroscopic coherence and cooperative light emission. Localization is one consequence of disorder that emerges from the recent experiments on perovskite nanocrystal superlattices. For example, Rainò *et al.* proposed the existence of superfluorescent domains within superlattices with an

estimated average number of coherently coupled $CsPbBr_3$ nanocrystals $N_{coupled} = 28$,[1] Blach *et al.* estimated $N_{coupled} = 3$.[8] More recently, Adl *et al.* measured a radiative enhancement factor in the range 1.2–11.0 for an estimated $N_{coupled} = 1000–40\,000$ $CsPbBr_3$ nanocrystals in similar superlattices.[9] Given that a single superlattice typically contains $N = 10^6–10^7$ nanocrystals, the yield of cooperativity is low and requires an explanation.

The $CsPbBr_3$ superlattices with $N = 10–10^4$ nanocrystals have been studied theoretically using a single-excitation model of superradiance.[19,20] These studies focused on the dependence of the superradiant rate enhancement on the total number of nanocrystals, center-to-center distance, aspect ratio (nanocubes vs nanoplatelets), a static energy disorder and the dimension of the superlattice (1D, 2D, 3D). Among the theoretical findings are predictions that arrays of smaller nanocubes are more resistant to thermal decoherence than arrays of larger nanocubes, and the emergence of cooperative robustness against decoherence in large 3D superlattices ($N > 10^3$). Considering the intense research interest in this topic, it is valuable to continue the systematic investigation of nanocrystal superlattice design parameters across different regimes of superradiance, particularly from weak to strong disorder, and in the Dicke limit or away from it.

In this work, we theoretically examine the effects of nanocube size, interparticle separation, energy and spatial disorder on the superradiance and on the spatial localization of the superradiant wave function in a 2D superlattice. We consider the enhancement of superradiance across different regimes of disorder, finding that optimizing the superradiance demands differing strategies of tuning nanocrystal parameters.

II. THEORETICAL MODEL

Let us consider the general case of a superlattice consisting of N_x, N_y and N_z nanocrystals along x, y and z axes respectively ($N = N_xN_yN_z$). Each nanocrystal is assumed to be a cube with an edge length L_{NC} and is covered with a homogeneous ligand shell of thickness L_{shell}. In the single-excitation regime, the system can be described by using the tight-binding Hamiltonian H_{rad}.[19,21]

$$H_{rad} = \sum_{n=1}^{N} \sum_{\alpha=x,y,z} E_n |n,\ \alpha\rangle\langle n,\ \alpha| + \sum_{\langle n,m\rangle}^{N} \sum_{\alpha,\beta} J_{mn}^{\alpha\beta} |m,\ \alpha\rangle\langle n,\ \beta| \quad (1)$$

The above Hamiltonian is applicable to both 3D and 2D superlattices, the latter by setting $N_z = 1$.

The first term in Eq. (1) describes a system of N uncoupled nanocrystals. The corresponding matrix consists of the 3×3 diagonal blocks in the basis of bright triplet states denoted by $|\alpha\rangle$. The complex diagonal term is

$$E_n = \hbar\left(\omega_0 - i\frac{\gamma_r}{2}\right) \quad (2)$$

where $\hbar\omega_0$ is the energy of bright exciton (without fine structure splitting) and γ_r is the radiative recombination rate of an exciton in a single nanocrystal.

The off-diagonal second term in Eq. (1)

$$J_{mn}^{\alpha\beta} = \frac{1}{2}\left(\Omega_{mn}^{\alpha\beta} - i\Gamma_{mn}^{\alpha\beta}\right) \quad (3)$$

originates from the radiative coupling between the nanocrystals in the superlattice.[19,21] The real and imaginary parts of J_{mn} are given as

$$\Omega_{mn}^{\alpha\beta} = \hbar\gamma_r\left(y_0(k_0 r_{mn})\hat{e}_\alpha \cdot \hat{e}_\beta - \frac{y_2(k_0 r_{mn})}{2} D_{mn}^{\alpha\beta}\right), \quad (4)$$

$$\Gamma_{mn}^{\alpha\beta} = \hbar\gamma_r\left(j_0(k_0 r_{mn})\hat{e}_\alpha \cdot \hat{e}_\beta - \frac{j_2(k_0 r_{mn})}{2} D_{mn}^{\alpha\beta}\right). \quad (5)$$

In the above, j_i/y_i denotes the spherical Bessel function of the first/second kind of order i. $D_{mn}^{\alpha\beta} = \hat{e}_\alpha \cdot \hat{e}_\beta - 3(\hat{e}_\alpha \cdot \hat{r}_{mn})(\hat{e}_\beta \cdot \hat{r}_{mn})$, $\hat{e}_\alpha$ is the unit vector in the α direction, $\hat{r}_{mn} = \vec{r}_{mn}/r_{mn}$ and $\vec{r}_{mn}$ is the position vector connecting the centers of the mth and nth nanocrystals. The resonant wave number $k_0 = \omega_0\sqrt{\varepsilon_{opt}}/c$ in which ε_{opt} is the optical dielectric constant of the material in the relevant frequency range.

The eigenvalues and eigenvectors of Hamiltonian H_{rad} can be obtained by diagonalizing of the corresponding $3N \times 3N$ matrix. The superradiant state is defined to be the eigenstate Ψ_{SR} of H_{rad} with the smallest (i.e. the most negative) imaginary part Γ_{SR}, which is defined as the superradiant radiative decay rate. Here we take into account only the radiative coupling and radiative recombination of excitons in the nanocrystals. Other recombination or energy transfer channels, for instance electron-phonon coupling or Auger-type processes, play the role of decoherence sources and are not considered in the current model.

The results presented in this manuscript focus on the described model applied to nanocubes with L_{NC} ranging from 5.0 to 20.0 nm, which are sizes representative of the $CsPbBr_3$ nanocubes spanning various confinement regimes and that have been synthesized with high uniformity, high photoluminescence quantum yield, and form close-packed assemblies in previous publications (see Refs. 22 and 23 for an overview).

III. RESULTS

A. Radiative enhancement in superlattice

We begin by examining the effects of the superlattice morphology and the nanocube size on the acceleration of the radiative decay of the superradiant state. Two superlattice morphologies of experimental relevance to $CsPbBr_3$ nanocubes are considered: a symmetric 2D monolayer $N_x \times N_y$ where $N_x = N_y$, and $N_z = 1$ [Fig. 1(a)][27–29] and a symmetric 3D superlattice consisting of $N_x \times N_y \times N_z$ nanocubes, $N_x = N_y = N_z$.[1–6,30]

For a total number of nanocubes N, the superradiant enhancement is defined as the ratio Γ_{SR}/γ_r between Γ_{SR} of the superlattice and the radiative rate of a single nanocrystal γ_r. The calculated Γ_{SR}/γ_r for 2D and 3D superlattice morphologies, each with $L_{NC} = 5.0$, 13.0 and 20.0 nm, are presented in Figs. 1(b)–1(d). The shell length was set to $L_{shell} = 1.5$ nm, a value typical of cesium oleate and oleylammonium bromide ligands used in the preparation of superfluorescent assemblies. For most nanocrystals of interest, many-body perturbation theory provides a reasonable description of the dependence of ω_0 and γ_r on L_{NC}.[24] More quantitative calculations of ω_0 and γ_r

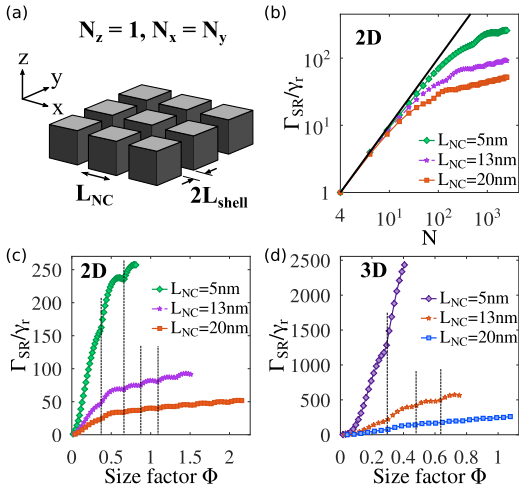

FIG. 1. (a) Sketch of the 2D superlattice. The superradiant (SR) rate enhancement for different lattice geometries and nanocube edge lengths (L_{NC} = 5, 13, and 20 nm, L_{shell} = 1.5 nm): (b) Γ_{SR}/γ_r vs total number of nanocrystals N for isotropic 2D superlattice, (c) Γ_{SR}/γ_r vs size factor $\Phi = d/\lambda$ (dimensionless) for isotropic 2D superlattice, where $d = N_x(L_{NC} + 2L_{shell})$, (d) Γ_{SR}/γ_r vs Φ for isotropic 3D superlattice. The vertical dashed lines indicate the points of plateauing behavior that are observed across the three nanocube sizes L_{NC}.

TABLE I. Physical parameters used in the calculations in this work for nanocrystals of sizes L_{NC} = 5.0, 13.0 and 20.0 nm. $\hbar\omega_0$ (eV): energy of bright exciton, γ_r^{-1} (ns): radiative decay lifetime of a single nanocrystal, δ_L (%): standard deviation for size distribution, δE (meV): inhomogeneous energy width due to size dispersion. The cuboidal nanocrystals are arranged into a cubic superlattice.

L_{NC} (nm)	$\hbar\omega_0$ (eV)[a]	γ_0^{-1} (ns)[b]	δ_L (%)	δE (meV)[c]
5.0	2.518	0.90	5	27.5
			10	51.1
			15	71.4
13.0	2.336	0.13	5	2.7
			10	4.9
			15	6.8
20.0	2.323	0.08	5	0.6
			10	1.1
			15	1.5

[a]From many-body perturbation theory calculations, Ref. 24.
[b]Extracted from BSE0 calculations, Ref. 25.
[c]Using the approximate analytical relation in Ref. 26.

vs L_{NC} based on configuration-interaction approach can be found in Ref. 25. For the range of nanocrystal sizes considered here, the nanocrystal energy $\hbar\omega_0$ varies from 2.32 to 2.52 eV, while the radiative decay times γ_r^{-1} varies from 0.1 to 0.9 ns, respectively, based on the calculations from these works.[24,25] More details can be found in Table I.

In panels (c) and (d) of Fig. 1, we defined the superlattice size factor $\Phi = d/\lambda$, where $d = N_x(L_{NC} + 2L_{shell})$ is the length of the superlattice, which is the distance covered by nanocubes along x direction, and $\lambda = 2\pi c/\omega_0\sqrt{\varepsilon_{opt}}$ is the resonant wavelength of the bright exciton. In other words, the dimensionless size factor Φ characterizes the relative size of the superlattice to the resonant wavelength. In the calculations, we consider superlattices containing a total number of nanocubes ranging from $N = 4$ to $N = 50^2$ for 2D and $N = 25^3$ for 3D case, which spans the Dicke limit ($\Phi \ll 1$) to the short wavelength limit ($\Phi \gg 1$). In the following, we note main observations from the results presented in Fig. 1.

First, similar trends in superradiant enhancement are observed between 2D and 3D superlattices [Figs. 1(c) and 1(d)]. Not only the 2D calculations still capture the key features of the structure-property relation with minuscule computation cost but also they permit a more transparent presentation of the wave functions (Fig. 4) for the discussion of superradiance localization in the later sections. Hence, we will focus on the results for 2D superlattices.

Second, the increase in the radiative enhancement, which grows approximately as $\sim N$ for a small number of nanocubes, shows a sub-linear behavior in N for larger superlattices.[19] This sub-linear behavior can be explained by the fact that the radiative coupling, Eqs. (4) and (5), attenuates for nanocubes that are further apart in a large superlattice. The increase is accompanied by shallow dips at the values indicated by the dashed lines in Figs. 1(c) and 1(d). In Ref. 31, similar dips were seen in dilute superradiant lattices where the interparticle spacing was comparable to the wavelength, and explained by geometric resonances when the lattice constant approaches certain critical values.

Third, for a fixed number N of nanocubes, a system with smaller L_{NC} exhibits stronger enhancement, i.e. larger Γ_{SR}/γ_r. This is particularly noticeable in the limit of small nanocube size, where the number of nanocubes that can be coupled within a region of size $\sim \lambda$ scales with their 2D packing density $(L_{NC} + 2L_{shell})^{-2}$. The optical transition energy $\hbar\omega_0$ (hence λ) is weakly size-dependent for the range of L_{NC} studied here. Therefore, the smaller L_{NC} (or smaller Φ) implies a stronger radiative coupling leading to larger Γ_{SR}/γ_r.[19]

Next, we systematically study the effect of shell length L_{shell} on the superradiant enhancement (Fig. 2). Two sizes of nanocubes L_{NC} = 5.0 and 20.0 nm, and five different shell lengths L_{shell} = 1.0, 10.0, 20.0, 40.0, and 80.0 nm were considered. The large L_{shell} resembles the situation of diluted 2D superlattice where the nanocrystal number density per unit volume is significantly reduced. Generally, as the L_{shell} increases, the superradiant enhancement is reduced to the point that, at large L_{shell} values, the superradiance enhancement is virtually independent of L_{NC} (e.g., L_{shell} = 40.0 and 80.0 nm, green squares, and orange triangles in Fig. 2, respectively).

As expected, a larger L_{shell} leads to a larger center-to-center distance between nanocubes. The larger distance weakens the radiative coupling [Eqs. (3)–(5)] and lowers the superradiant enhancement. Intriguingly, the effect of increasing L_{shell} onto the superradiant wave function is not intuitive.

The color plots in Fig. 4 show the total norm of the superradiant wave functions, obtained by summing over norms of the x, y, and z components of the $3N$ complex eigenvector, at each site of the $N_x \times N_y$ superlattice. For the case where L_{shell} = 1.0 nm and L_{NC} = 5.0 nm, the superradiant wave function spreads out and delocalizes over the entire superlattice, resulting

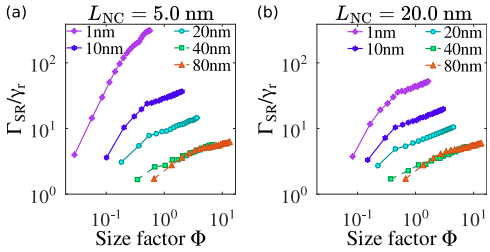

FIG. 2. Superradiant enhancement Γ_{SR}/γ_r vs the size factor Φ for two sizes, (a) L_{NC} = 5.0 nm and (b) L_{NC} = 20.0 nm for various shell lengths L_{shell} = 1.0, 10.0, 20.0, 40.0 and 80.0 nm. Generally, as the shell length increases, the enhancement Γ_{SR}/γ_r decreases. For large L_{shell}, the effect of the nanocrystal size becomes less important.

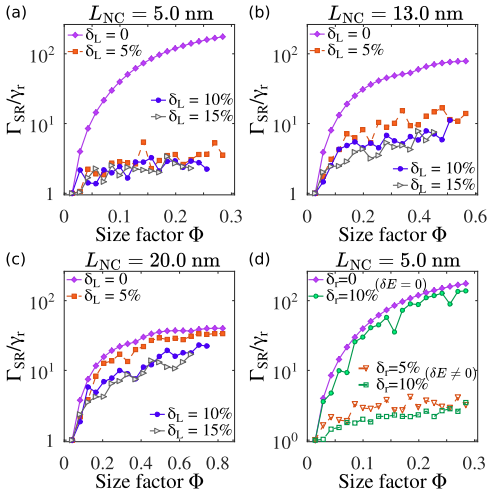

FIG. 3. Radiative enhancement Γ_{SR}/γ_r vs the size factor Φ with only energy disorder [panels (a)–(c), δ_r = 0] and some random variation in the positions of NC centers [panel (d)]. (a) L_{NC} = 5.0 nm, (b) L_{NC} = 13.0 nm, (c) L_{NC} = 20.0 nm, (d) L_{NC} = 5.0 nm without (δE = 0, filled symbols) and with ($\delta E \neq 0$, empty symbols) energy disorder. For each size, the values of the energy width δE for each value of δ_L can be found in Table I. Shell length L_{shell} = 1.0 nm in all calculations. Energy disorder δE is characterized by size dispersion δ_L (dimensionless). Spatial randomness has Gaussian distribution of width δ_r.

in the largest Γ_{SR}/γ_r. The biggest nanocubes, L_{NC} = 20.0 nm, with the same L_{shell} = 1.0 nm, exhibit the delocalization of Ψ_{SR} to a lesser extent, resulting in reduced Γ_{SR}/γ_r (see Fig. 2 for comparison). For a large L_{shell} = 40.0 nm, the N – particle wave function Ψ_{SR} fragments into several "pockets" of superradiance [Figs. 4(c) and 4(d)] for both L_{NC} sizes. The unexpected superradiance localization in a perfect superlattice is attributed to the weakened radiative coupling. To overcome the localization, strategies for enhancing radiative coupling are needed. For example, introducing a cavity may help overcome the delocalization through Purcell enhancement.[32]

B. Effect of energy disorder

In this subsection, we consider the role of static energy disorder stemming from the size dispersion of nanocubes prepared by chemical syntheses. We note that there are other contributions, such as different surface passivation, shape variation, and dynamic disorder, to the energy dispersion, even at low temperatures.[15] Our choice to investigate the dependence of Γ_{SR}/γ_0 on δ_L and δE is based on the assumption that size dispersion captures the essence of static disorder in colloidal nanocrystals.

For an ensemble of average size L_{NC}, the size dispersion is characterized by the dimensionless quantity $\delta_L = \delta L_{NC}/L_{NC}$ where δL_{NC} is the standard deviation in the size distribution. In this paper, we use the same method based on power series expansion as in the supplementary material of Ref. 26 to estimate the δ_L – dependent energy width δE for inhomogeneous broadening. To capture the effect of this energetic variation among the nanocubes, we introduce an additional term ΔE_n that follows the Gaussian distribution

$$\mathcal{G}(x) = \frac{1}{\sqrt{2\pi}\,\delta E}\exp\left[-\frac{1}{2}\frac{x^2}{(\delta E)^2}\right], \tag{6}$$

applied to the diagonal energy E_n in Eq. (2).

It is customary to use batches of colloidal nanocrystals with a narrow size distribution (δ_L of 10% or less) to produce well-ordered superlattices.[33,34] The reported average sizes for $CsPbBr_3$ nanocubes characterized with electron microscopy yield δL_{NC} in the range of 0.5–1 nm for L_{NC} = 5–20 nm.[35,36] This is equivalent to a variation of δ_L in the range from 5 to 10%. Therefore, we study the effect of the static energy disorder on the superradiant enhancement Γ_{SR}/γ_r for various δ_L as shown in Figs. 3(a)–3(c) and 5.

For all nanocube sizes L_{NC}, the energy disorder clearly diminishes the superradiant enhancement. Generally, in a more polydispersed sample, the larger energy variation among the constituent nanocubes significantly reduces the effect of the coupling defined in Eq. (3) of the total Hamiltonian. Hence, the eigenstates, especially the superradiant solution, in Eq. (1) are pushed towards those of an uncoupled system. For superlattices made of smaller nanocubes, the same size dispersion δ_L results in a larger energy width δE and, thus, more dramatic reduction in radiative enhancement compared to larger nanocubes. Notably, for the case of L_{NC} = 5.0 nm in Fig. 3(a), a level of size dispersion around 5% (δE = 27.5 meV) is sufficient to quench the cooperative effect. On the other hand, for L_{NC} = 20.0 nm, a part of the cooperative enhancement at δ_L = 15% (δE = 1.5 meV) is still retained in the superradiant state.

The influence of size dispersion on superradiance can be understood and visualized from the perspective of wave function distribution over the superlattice. Panels (e) and (f) of Fig. 4 show, in the case with energy disorder determined by δ_L = 10%, the total norm of the wave functions Ψ_{SR} of superlattices made of nanocubes with L_{NC} = 5.0 nm [panel (e)] and L_{NC} = 20.0 nm [panel (f)]. We note an important observation from a quick comparison with the case without energy disorder (δ_L = 0% implying δE = 0) in panels (a) and (b) of Fig. 4: the static energy disorder alters the localization property of the N – nanocube wave function from being delocalized over the superlattice to being localized on several nanocubes. The localization of the superradiant wave function gets stronger with the bigger value of energy width δE, making smaller nanocubes more susceptible to the effects of disorder than larger nanocubes.

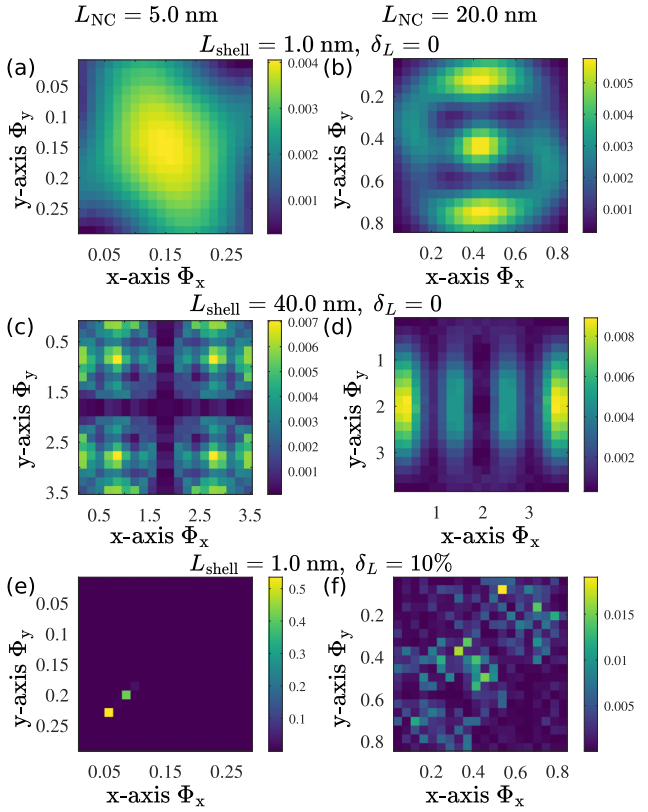

FIG. 4. Distribution of superradiant wave functions over the 2D superlattice for L_{NC} = 5.0 nm (left panels) and L_{NC} = 20.0 nm (right panels). For each size, three cases are covered: no energy disorder [panels (a)–(b)], i.e. $\delta_L = 0$ and L_{shell} = 1.0 nm, $\delta_L = 0$ and large distance between NCs where L_{shell} = 40.0 nm [panels (c)–(d)] and with energy disordered derived from size dispersion δ_L = 10% and L_{shell} = 1.0 nm [panels (e)–(f)]. Large nanocrystal separation leads to the formation of smaller pockets of superradiance. Large static energy disorder results in the destruction of cooperative behaviour due to localization of the wave function.

The effect of energy disorder saturates past a certain point, with disorder greater than δ_L = 10%–15% showing similar emission characteristics in our simulations. Even in this limit, when energy disorder is large enough to cause large reductions in the superradiance rate, emission rates are still expected to increase with the superlattice size factor Φ, as seen in Figs. 3(a)–3(c), albeit at a slower rate than in a perfect superlattice with $\delta_L = 0$. This is surprising because cooperative superradiance is destroyed by localization in this limit [Figs. 4(e) and 4(f)]. Instead, increasing the superlattice size factor in the presence of strong disorder increases the probability of the formation of local regions of strong emission, arising from the concerted local fluctuation of the diagonal energies E_n. That explains the cooperative robustness to disorder reported by Ghonge *et al.*[20]

C. Effect of spatial displacement

So far, only the effect of static energy disorder has been considered, while the center-to-center distance $L_{NC} + 2L_{shell}$ between the adjacent nanocubes remains identical. However, the random size distribution also affects the particle arrangement within a superlattice and displaces the centers of nanocubes out of their perfect positions. X-ray diffraction studies of $CsPbBr_3$ nanocube superlattices point out small, ~1 Å, fluctuations in center-to-center distances between nanocubes, suggesting the "structural coherence" could be a factor underlying the emergence of collective optical properties.[37,38] To simulate the effect of spatial displacement of nanocubes relative to each other in the superlattice, the position vector $\vec{r}_{mn}$, from the center of the mth to the center of the nth nanocube, is replaced by

$$\vec{\tilde{r}}_{mn} = \vec{r}_{mn} + \Delta\vec{r}_{mn}, \tag{7}$$

where $\Delta\vec{r}_{mn}$ is a random vector belonging to a Gaussian distribution of width δ_r, and δ_r is the dimensionless quantity that characterizes the degree of displacement [similar to Eq. (6)].

Figure 3(d) shows the results of Γ_{SR}/γ_r for the case of superlattices with $\delta_r = 0$, $\delta E = 0$ (filled purple diamonds), with only random displacement δ_r = 10% and no energy disorder $\delta E = 0$ (filled green circles), with random displacement and energy disorder, $\delta_r = \delta_L$ = 5% (empty red triangles) and $\delta_r = \delta_L$ = 10% (empty green squares). The choice $\delta_r = \delta_L$ is motivated by the fact that the spatial displacement is due to the size dispersion. Without energy disorder, some slight reduction is observed in the radiative enhancement due to the randomness in nanocube-to-nanocube distance $\vec{\tilde{r}}_{mn}$. Nonetheless, the most significant impact of size dispersion on the superradiant enhancement Γ_{SR}/γ_r occurs through the energy disorder [Eq. (6)] and not through the imperfect spatial arrangement of nanocubes, especially in superlattices made of nanocubes in strong or intermediate confinement regime.

IV. DISCUSSION

The above results have uncovered competing effects of the nanocube size L_{NC} onto superradiant enhancement Γ_{SR}/γ_r. On the one hand, superradiance from small nanocubes is enhanced due to the higher packing density and shorter center-to-center distances (Figs. 1 and 2). On the other hand, small nanocubes are susceptible to energy disorder and show strongly suppressed superradiance (Fig. 4). For instance, the large value of δE for the case of L_{NC} = 5.0 nm leads to an almost complete quenching of Γ_{SR}/γ_r and the localization of the wave function Ψ_{SR} onto a few nanocube sites (Anderson localization).[8,39–41] The degree of localization is controlled by the energy width δE [Figs. 4(e) and 4(f)] and manifests the order-disorder transition in a nanocrystal superlattice. These results suggest a possible explanation for minuscule values of $N_{coupled}$ in recent experiments.[7,8]

To illustrate the point and showcase the immediate utility of the model for interpreting experimental results, we extracted experimental parameters from Refs. 7 and 8 and ran the calculations. In the first case, using L_{NC} = 9.0 nm, L_{shell} = 1.5 nm, and an energy width δE = 7.8 meV,[8] we obtained, from the radiative Hamitonian, the enhancement factors ranging from 4.7 to 6.5 for 3D superlattices with N = 5 × 5 × 5 to 12 × 12 × 12. The calculated enhancement is higher than the reported factor of 2.7, and the difference is reconcilable by a slightly higher δE. In the second case, for 2D superlattices with N = 40 × 40 and L_{NC} = 3.8 nm, an enhancement factor of 1.9 in the superradiant decay rate was

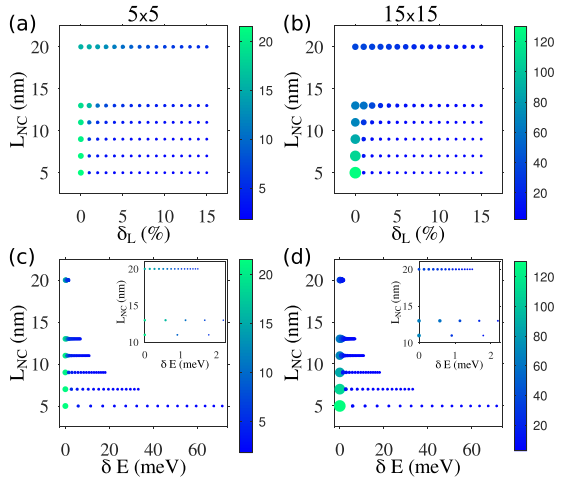

FIG. 5. Radiative enhancement Γ_{SR}/γ_r (color map) vs the size L_{NC} of nanocubes and size dispersion δ_L/energy width δE for 5 × 5 superlattices [panels (a), (c)] and 15 × 15 superlattices [panels (b), (d)]. The result in each panel is an average over 48 realizations of energy disorder. The dot size was scaled linearly with the value of Γ_{SR}/γ_r. Note the reversed trend of the radiative enhancement vs L_{NC} as the size dispersion moves away from $\delta_L = 0$.

calculated when the ligand length L_{shell} was changed from 1.5 nm (oleylammonium bromide, experimental $\delta E = 32.3$ meV) to 0.35 nm (sodium bromide, $\delta E = 24.2$ meV), which is close to the experimental ratio of 1.5 between the fast-components of the decay rates.[7]

How to counteract the punishing effect of energy disorder? One strategy is to increase the L_{NC} hence reducing the impact of size dispersion δ_L. Figure 5 maps the radiative enhancement Γ_{SR}/γ_r as a function of δ_L (upper panels) or δE (lower panels) for $N_x \times N_y = 5 \times 5$ ($\Phi \ll 1$, the Dicke regime) and 15 × 15 superlattices. The strategy for maintaining superradiance in the face of large δ_L is to shift to the upper part of the map (albeit with a modest $\Gamma_{SR}/\gamma_r = 5$–20), in other words, use larger nanocubes (L_{NC} = 10–20 nm). Under near-perfect conditions, the smaller nanocubes (L_{NC} = 5–10 nm) are clearly preferred as they deliver the largest radiative enhancement of $\Gamma_{SR}/\gamma_r = 20$–120.

The employed theoretical model is rooted in molecular aggregates[21] and it is instructive to compare the described effects of disorder in nanocubes with molecules. Fidder *et al.* computed the effects of Gaussian distribution of transition energies (δE, diagonal disorder) and inter-molecular distances (off-diagonal disorder) on superradiance for a linear molecular aggregate in $\Phi \ll 1$ regime.[42] Since size distribution is not a concern for molecules, the δE was set as a fraction of dipole-dipole interaction energy between neighbours. Both types of disorder were found to result in excitation localization to the ends of the chain. However, the quenching of radiative enhancement was found to be more sensitive to the off-diagonal disorder rather than the diagonal disorder, with one reason being the formation of strongly-interacting dimers. Jang and Silbey found that both types of disorder matter for excitation localization in a model of a molecular ring of light-harvesting complex 2,[43] with either one capable of dominating localization depending on their magnitude and correlation. In contrast to detrimental effect of disorder in identical emitters, Moix *et al.* considered a model of Fenna–Matthews–Olson complex with a built-in energy transfer (a biased system), finding that diagonal disorder enhances delocalization.[44] The brief comparison with molecular aggregates indicates that the effects of the disorder on radiative enhancement and localization are not axiomatic and depend on the specific emitter configuration and properties of the system. Continuing to adapt various scenarios from molecular aggregates to nanocrystal superlattices offers exciting avenues for future research.

Next, it is important to revisit several fundamental assumptions of the theoretical model. The Hamiltonian defined Eq. (1) is applicable in the ideal case where all dipoles are aligned, i.e. in-phase, and isotropic where the x, y and z components of the optical dipoles have the same oscillator strength. Including the phase decoherence between the optical dipoles or the anisotropy of the optical dipole may be essential to understand more comprehensively the superradiant behaviour.[45] So far, only the single-excitation regime has been considered.[19–21] At high excitation intensities, the formation of multiple excitons is likely,[46,47] in which the single-excitation Hamiltonian is no longer valid. In this case, a new framework to describe the system beyond single excitation remains to be developed for nanocrystal superlattices.

Finally, it is valuable to put the results in the context of the available superlattices and $CsPbBr_3$ nanocubes, and discuss the feasibility of future experiments. Current literature suggests a few viable methods for producing 2D superlattices. For example, irregular finite-sized monolayers of $CsPbBr_3$ nanocrystals have been made by solvent evaporation[27] and extended 2D monolayers ($\Phi \gg 1$) of close-packed $CsPbBr_3$ nanocrystals (L_{NC} = 10–15 nm) were achieved by solvent vapor annealing.[28] In a demonstration of control over lateral dimensions of 2D superlattices, Cohen *et al.* fabricated sub-micron ($\Phi \geq 1$) islands of $CsPbBr_3$ nanocrystals with $L_{NC} = 9.7 \pm 2.1$ nm by electrohydrodynamic inkjet printing.[29] The latest generations of small colloidal $CsPbBr_3$ nanocrystals with $L_{NC} = 5$ nm ($\delta_L = 7.5\%$)[48] and large ones with $L_{NC} = 19.8 \pm 1.7$ nm[49] have been reported as high-quality single photon emitters and are feasible building blocks for superradiant assemblies. However, the reported size distributions need to be substantially reduced to avoid localization, as suggested by our model.

From a spectroscopic point of view, the 10– to 10^4–fold acceleration of radiative decay suggests superradiance timescales in the range from tens of femtoseconds (fs) to tens of picoseconds (ps) (using 200–400 ps radiative lifetimes of $CsPbBr_3$ nanocubes near 4 K[50–53]). In the lower limit (i.e. tens of fs), the timescale of superradiance becomes comparable to that of the exciton formation.[54] In the intermediate range (1–2 ps), superradiance is comparable to the carrier cooling (0.3–0.7 ps in 8 nm $CsPbBr_3$ nanocubes at room temperature)[55] and the polaron formation (0.8 ps in a single crystal $CsPbBr_3$ at room temperature).[56] Given the typical duration of ultrashort laser pulses (10–100 fs), detecting superradiance requires femtosecond spectroscopies such as transient absorption or multi-dimensional spectroscopies. On the higher end of the range (tens of ps), the superradiance falls within the time resolution of state-of-the-art commercial streak cameras and could be probed by time-resolved photoluminescence.[1–3,6]

V. CONCLUSIONS

We have presented a systematic theoretical investigation of the superradiant Hamiltonian for 2D nanocrystal superlattices and argued that they are feasible testbeds of collective phenomena. Although the focus of the study is on the lead halide perovskite nanocubes, the model can be easily adapted to study nanoscale emitters of other materials. The results presented here are in agreement with the earlier works of Mattiotti *et al.* and Ghonge *et al.*, who studied superradiance and its suppression by energy disorder and thermal decoherence using the same model.[19,20]

The reported calculations provided valuable insights into the non-trivial dependence of superradiance on experimentally relevant parameters such as L_{NC}, L_{shell}, δ_E, and δ_r, their role and interplay in excitation localization. The results clearly show that, in pursuing cooperative effects, having as identical nanocubes as possible in the superlattice is more important than achieving a perfect spatial order. And if perfect nanocubes are not possible, larger imperfect nanocubes are preferred over smaller ones. These predictions await experimental verifications and we are optimistic about the possibility of such tests given the interest in these materials and superradiance phenomena.

ACKNOWLEDGMENTS

L.Z.T. was supported by the Molecular Foundry, a DOE Office of Science User Facility supported by the Office of Science of the U.S. Department of Energy under Contract No. DE-AC02-05CH11231. This research used resources of the National Energy Research Scientific Computing Center, a DOE Office of Science User Facility supported by the Office of Science of the U.S. Department of Energy under Contract No. DE-AC02-05CH11231.

D.B. was funded by the European Union (ERC Starting Grant PROMETHEUS, project No. 101039683). Views and opinions expressed are however those of the authors only and do not necessarily reflect those of the European Union or the European Research Council Executive Agency. Neither the European Union nor the granting authority can be held responsible for them.

AUTHOR DECLARATIONS

Conflict of Interest

The authors have no conflicts to disclose.

Author Contributions

T. P. Tan Nguyen: Conceptualization (equal); Data curation (lead); Formal analysis (equal); Investigation (equal); Methodology (equal); Resources (equal); Software (lead); Validation (equal); Visualization (lead); Writing – original draft (equal); Writing – review & editing (equal). **Liang Z. Tan**: Conceptualization (equal); Formal analysis (equal); Methodology (equal); Software (equal); Supervision (equal); Writing – review & editing (equal). **Dmitry Baranov**: Conceptualization (equal); Data curation (supporting); Formal analysis (supporting); Funding acquisition (lead); Investigation (equal); Methodology (supporting); Project administration (lead); Resources (equal); Supervision (equal); Validation (equal); Writing – original draft (equal); Writing – review & editing (equal).

DATA AVAILABILITY

The data that support the findings of this study are available from the corresponding authors upon reasonable request.

REFERENCES

[1]G. Rainò, M. A. Becker, M. I. Bodnarchuk, R. F. Mahrt, M. V. Kovalenko, and T. Stöferle, "Superfluorescence from lead halide perovskite quantum dot superlattices," Nature **563**, 671–675 (2018).
[2]C. Zhou, Y. Zhong, H. Dong, W. Zheng, J. Tan, Q. Jie, A. Pan, L. Zhang, and W. Xie, "Cooperative excitonic quantum ensemble in perovskite-assembly superlattice microcavities," Nat. Commun. **11**, 329 (2020).
[3]F. Krieg, P. C. Sercel, M. Burian, H. Andrusiv, M. I. Bodnarchuk, T. Stöferle, R. F. Mahrt, D. Naumenko, H. Amenitsch, G. Rainò, and M. V. Kovalenko, "Monodisperse long-chain sulfobetaine-capped $CsPbBr_3$ nanocrystals and their superfluorescent assemblies," ACS Cent. Sci. **7**, 135–144 (2020).
[4]I. Cherniukh, G. Rainò, T. V. Sekh, C. Zhu, Y. Shynkarenko, R. A. John, E. Kobiyama, R. F. Mahrt, T. Stöferle, R. Erni, M. V. Kovalenko, and M. I. Bodnarchuk, "Shape-directed co-assembly of lead halide perovskite nanocubes with dielectric nanodisks into binary nanocrystal superlattices," ACS Nano **15**, 16488–16500 (2021).
[5]I. Cherniukh, M. V. Rainò, T. Stöferle, M. Burian, A. Travesset, G. Naumenko, H. Amenitsch, R. Erni, R. F. Mahrt, M. I. Bodnarchuk, and D. Kovalenko, "Perovskite-type superlattices from lead halide perovskite nanocubes," Nature **593**, 535–542 (2021).
[6]Y. Zhong, C. Zhou, L. Hou, J. Li, W. Xie, H. Dong, and L. Zhang, "Ultrafast optical properties of cavity-enhanced superfluorescence," Adv. Opt. Mater. **10**, 2102290 (2022).
[7]X. Tang, D. Rossi, J. Cheon, and D. H. Son, "Effects of electronic coupling on bright and dark excitons in a 2D array of strongly confined $CsPbBr_3$ quantum dots," Chem. Mater. **34**, 7181–7189 (2022).
[8]D. D. Blach, V. A. Lumsargis, D. E. Clark, C. Chuang, K. Wang, L. Dou, R. D. Schaller, J. Cao, C. W. Li, and L. Huang, "Superradiance and exciton delocalization in perovskite quantum dot superlattices," Nano Lett. **22**, 7811–7818 (2022).
[9]H. P. Adl, S. Gorji, G. Muñoz-Matutano, A. F. Gualdrón-Reyes, I. Suárez, V. S. Chirvony, I. Mora-Seró, and J. P. Martínez-Pastor, "Superradiance emission and its thermal decoherence in lead halide perovskites superlattices," Adv. Opt. Mater. **11**, 2202497 (2023).
[10]X. Li, Z. Xue, X. Chen, X. Qiao, G. Mo, W. Bu, B. Guan, and T. Wang, "Printable assemblies of perovskite nanocubes on meter-scale panel," Sci. Adv. **8**, eadd1559 (2022).
[11]R. H. Dicke, "Coherence in spontaneous radiation processes," Phys. Rev. **93**, 99 (1954).
[12]R. Bonifacio and L. A. Lugiato, "Cooperative radiation processes in two-level systems: Superfluorescence," Phys. Rev. A **11**, 1507 (1975).
[13]N. Skribanowitz, I. Herman, J. MacGillivray, and M. Feld, "Observation of Dicke superradiance in optically pumped HF gas," Phys. Rev. Lett. **30**, 309 (1973).
[14]M. Gross, C. Fabre, P. Pillet, and S. Haroche, "Observation of near-infrared Dicke superradiance on cascading transitions in atomic sodium," Phys. Rev. Lett. **36**, 1035 (1976).
[15]H. A. Nguyen, G. Dixon, F. Y. Dou, S. Gallagher, S. Gibbs, D. M. Ladd, E. Marino, J. C. Ondry, J. P. Shanahan, E. S. Vasileiadou, S. Barlow, D. R. Gamelin, D. S. Ginger, D. M. Jonas, M. G. Kanatzidis, S. R. Marder, D. Morton, C. B. Murray, J. S. Owen, D. V. Talapin, M. F. Toney, and B. M. Cossairt, "Design rules for obtaining narrow luminescence from semiconductors made in solution," Chem. Rev. **123**, 7890–7952 (2023).
[16]J. S. van der Burgt, J. J. Geuchies, B. van der Meer, H. Vanrompay, D. Zanaga, Y. Zhang, W. Albrecht, A. V. Petukhov, L. Filion, S. Bals, I. Swart, and D. Vanmaekelbergh, "Cuboidal supraparticles self-assembled from cubic $CsPbBr_3$ perovskite nanocrystals," J. Phys. Chem. C **122**, 15706–15712 (2018).

[17]S. Toso, D. Baranov, D. Altamura, F. Scattarella, J. Dahl, X. Wang, S. Marras, A. P. Alivisatos, A. Singer, C. Giannini, and L. Manna, "Multilayer diffraction reveals that colloidal superlattices approach the structural perfection of single crystals," ACS Nano **15**, 6243–6256 (2021).
[18]D. Lapkin, C. Kirsch, J. Hiller, D. Andrienko, D. Assalauova, K. Braun, J. Carnis, Y. Y. Kim, M. Mandal, A. Maier, A. J. Meixner, N. Mukharamova, M. Scheele, F. Schreiber, M. Sprung, J. Wahl, S. Westendorf, I. A. Zaluzhnyy, and I. A. Vartanyants, "Spatially resolved fluorescence of caesium lead halide perovskite supercrystals reveals quasi-atomic behavior of nanocrystals," Nat. Commun. **13**, 892 (2022).
[19]F. Mattiotti, M. Kuno, F. Borgonovi, B. Jankó, and G. L. Celardo, "Thermal decoherence of superradiance in lead halide perovskite nanocrystal superlattices," Nano Lett. **20**, 7382–7388 (2020).
[20]S. Ghonge, D. Engel, F. Mattiotti, G. L. Celardo, M. Kuno, and B. Jankó, "Enhanced robustness and dimensional crossover of superradiance in cuboidal nanocrystal superlattices," Phys. Rev. Res. **5**, 023068 (2022).
[21]J. Grad, G. Hernandez, and S. Mukamel, "Radiative decay and energy transfer in molecular aggregates: The role of intermolecular dephasing," Phys. Rev. A **37**, 3835–3846 (1988).
[22]A. Dey, J. Ye, A. De, E. Debroye, S. K. Ha, E. Bladt, A. S. Kshirsagar, Z. Wang, J. Yin, Y. Wang, L. N. Quan, F. Yan, M. Gao, X. Li, J. Shamsi, T. Debnath, M. Cao, M. A. Scheel, S. Kumar, J. A. Steele, M. Gerhard, L. Chouhan, K. Xu, X.-g. Wu, Y. Li, Y. Zhang, A. Dutta, C. Han, I. Vincon, A. L. Rogach, A. Nag, A. Samanta, B. A. Korgel, C.-J. Shih, D. R. Gamelin, D. H. Son, H. Zeng, H. Zhong, H. Sun, H. V. Demir, I. G. Scheblykin, I. Mora-Seró, J. K. Stolarczyk, J. Z. Zhang, J. Feldmann, J. Hofkens, J. M. Luther, J. Pérez-Prieto, L. Li, L. Manna, M. I. Bodnarchuk, M. V. Kovalenko, M. B. J. Roeffaers, N. Pradhan, O. F. Mohammed, O. M. Bakr, P. Yang, P. Müller-Buschbaum, P. V. Kamat, Q. Bao, Q. Zhang, R. Krahne, R. E. Galian, S. D. Stranks, S. Bals, V. Biju, W. A. Tisdale, Y. Yan, R. L. Z. Hoye, and L. Polavarapu, "State of the art and prospects for halide perovskite nanocrystals," ACS Nano **15**, 10775–10981 (2021).
[23]Z. Liu, X. Qin, Q. Chen, T. Jiang, Q. Chen, and X. Liu, "Metal–halide perovskite nanocrystal superlattice: Self-assembly and optical fingerprints," Adv. Mater. **35**, 2209279 (2023).
[24]T. Nguyen, S. Blundell, and C. Guet, "One-photon absorption by inorganic perovskite nanocrystals: A theoretical study," Phys. Rev. B **101**, 195414 (2020).
[25]S. A. Blundell and C. Guet, "All-order correlation of single excitons in nanocrystals using a $k \cdot p$ envelope-function approach: Application to lead halide perovskites," Phys. Rev. B **105**, 155420 (2022).
[26]Q. A. Akkerman, T. P. T. Nguyen, S. C. Boehme, F. Montanarella, D. N. Dirin, P. Wechsler, F. Beiglböck, G. Rainò, R. Erni, C. Katan, J. Even, and M. V. Kovalenko, "Controlling the nucleation and growth kinetics of lead halide perovskite quantum dots," Science **377**, 1406–1412 (2022).
[27]M. J. Jurow, T. Lampe, E. Penzo, J. Kang, M. A. Koc, T. Zechel, Z. Nett, M. Brady, L.-W. Wang, A. P. Alivisatos, S. Cabrini, W. Brütting, and Y. Liu, "Tunable anisotropic photon emission from self-organized $CsPbBr_3$ perovskite nanocrystals," Nano Lett. **17**, 4534–4540 (2017).
[28]B. K. Patra, H. Agrawal, J.-Y. Zheng, X. Zha, A. Travesset, and E. C. Garnett, "Close-packed ultrasmooth self-assembled monolayer of $CsPbBr_3$ perovskite nanocubes," ACS Appl. Mater. Interfaces **12**, 31764–31769 (2020).
[29]T. A. Cohen, D. Sharp, K. T. Kluherz, Y. Chen, C. Munley, R. T. Anderson, C. J. Swanson, J. J. D. De Yoreo, C. K. Luscombe, A. Majumdar, D. R. Gamelin, and J. D. Mackenzie, "Direct patterning of perovskite nanocrystals on nanophotonic cavities with electrohydrodynamic inkjet printing," Nano Lett. **22**, 5681–5688 (2022).
[30]D. Baranov, S. Toso, M. Imran, and L. Manna, "Investigation into the photoluminescence red shift in cesium lead bromide nanocrystal superlattices," J. Phys. Chem. Lett. **10**, 655–660 (2019).
[31]S. J. Masson and A. Asenjo-Garcia, "Universality of dicke superradiance in arrays of quantum emitters," Nat. Commun. **13**, 2285 (2022).
[32]R. Fleury and A. Alù, "Enhanced superradiance in epsilon-near-zero plasmonic channels," Phys. Rev. B **87**, 201101 (2013).
[33]C. B. Murray, C. R. Kagan, and M. G. Bawendi, "Synthesis and characterization of monodisperse nanocrystals and close-packed nanocrystal assemblies," Annu. Rev. Mater. Sci. **30**, 545–610 (2000).
[34]C. Collier, T. Vossmeyer, and J. R. Heath, "Nanocrystal superlattices," Annu. Rev. Phys. Chem. **49**, 371–404 (1998).
[35]M. C. Brennan, J. E. Herr, T. S. Nguyen-Beck, J. Zinna, S. Draguta, S. Rouvimov, J. Parkhill, and M. Kuno, "Origin of the size-dependent Stokes shift in $CsPbBr_3$ perovskite nanocrystals," J. Am. Chem. Soc. **139**, 12201–12208 (2017).
[36]M. Imran, P. Ijaz, D. Baranov, L. Goldoni, U. Petralanda, Q. Akkerman, A. L. Abdelhady, M. Prato, P. Bianchini, I. Infante, and L. Manna, "Shape-pure, nearly monodispersed $CsPbBr_3$ nanocubes prepared using secondary aliphatic amines," Nano Lett. **18**, 7822–7831 (2018).
[37]S. Toso, D. Baranov, U. Filippi, C. Giannini, and L. Manna, "Collective diffraction effects in perovskite nanocrystal superlattices," Acc. Chem. Res. **56**, 66–76 (2023).
[38]F. Bertolotti, A. Vivani, F. Ferri, P. Anzini, A. Cervellino, M. I. Bodnarchuk, G. Nedelcu, C. Bernasconi, M. V. Kovalenko, N. Masciocchi, and A. Guagliardi, "Size segregation and atomic structural coherence in spontaneous assemblies of colloidal cesium lead halide nanocrystals," Chem. Mater. **34**, 594–608 (2022).
[39]G. L. Celardo, A. Biella, L. Kaplan, and F. Borgonovi, "Interplay of superradiance and disorder in the Anderson model," Fortschr. Phys. **61**, 250–260 (2013).
[40]G. L. Celardo, G. G. Giusteri, and F. Borgonovi, "Cooperative robustness to static disorder: Superradiance and localization in a nanoscale ring to model light-harvesting systems found in nature," Phys. Rev. B **90**, 075113 (2014).
[41]J. P. Philbin, J. Kelly, L. Peng, I. Coropceanu, A. Hazarika, D. V. Talapin, E. Rabani, X. Ma, and P. Narang, "Room temperature single-photon superfluorescence from a single epitaxial cuboid nano-heterostructure," arXiv:2104.06452 (2021).
[42]H. Fidder, J. Knoester, and D. A. Wiersma, "Optical properties of disordered molecular aggregates: A numerical study," J. Chem. Phys. **95**, 7880–7890 (1991).
[43]S. Jang, S. E. Dempster, and R. J. Silbey, "Characterization of the static disorder in the b850 band of LH2," J. Phys. Chem. B **105**, 6655–6665 (2001).
[44]J. M. Moix, Y. Zhao, and J. Cao, "Equilibrium-reduced density matrix formulation: Influence of noise, disorder, and temperature on localization in excitonic systems," Phys. Rev. B **85**, 115412 (2012).
[45]K. Cong, Q. Zhang, Y. Wang, G. T. Noe, A. Belyanin, and J. Kono, "Dicke superradiance in solids," J. Opt. Soc. Am. B **33**, C80–C101 (2016).
[46]P. Tamarat, L. Hou, J.-B. Trebbia, A. Swarnkar, L. Biadala, Y. Louyer, M. I. Bodnarchuk, M. V. Kovalenko, J. Even, and B. Lounis, "The dark exciton ground state promotes photon-pair emission in individual perovskite nanocrystals," Nat. Commun. **11**, 6001 (2020).
[47]Z. Wang, A. Rasmita, G. Long, D. Chen, C. Zhang, O. G. Garcia, H. Cai, Q. Xiong, and W.-b. Gao, "Optically driven giant superbunching from a single perovskite quantum dot," Adv. Opt. Mater. **9**, 2100879 (2021).
[48]S. C. Boehme, M. I. Bodnarchuk, M. Burian, F. Bertolotti, I. Cherniukh, C. Bernasconi, C. Zhu, R. Erni, H. Amenitsch, D. Naumenko, H. Andrusiv, N. Semkiv, R. A. John, A. Baldwin, K. Galkowski, N. Masciocchi, S. D. Stranks, G. Rainò, A. Guagliardi, and M. V. Kovalenko, "Strongly confined $CsPbBr_3$ quantum dots as quantum emitters and building blocks for rhombic superlattices," ACS Nano **17**, 2089–2100 (2023).
[49]A. E. K. Kaplan, C. J. Krajewska, A. H. Proppe, W. Sun, T. Sverko, D. B. Berkinsky, H. Utzat, and M. G. Bawendi, "Hong–Ou–Mandel interference in colloidal $CsPbBr_3$ perovskite nanocrystals," Nat. Photonics **17**, 775–780 (2023).
[50]F. Hu, H. Zhang, C. Sun, C. Yin, B. Lv, C. Zhang, W. W. Yu, X. Wang, Y. Zhang, and M. Xiao, "Superior optical properties of perovskite nanocrystals as single photon emitters," ACS Nano **9**, 12410–12416 (2015).
[51]G. Rainò, G. Nedelcu, L. Protesescu, M. I. Bodnarchuk, M. V. Kovalenko, R. F. Mahrt, and T. Stöferle, "Single cesium lead halide perovskite nanocrystals at low temperature: Fast single-photon emission, reduced blinking, and exciton fine structure," ACS Nano **10**, 2485–2490 (2016).
[52]H. Utzat, W. Sun, A. E. K. Kaplan, F. Krieg, M. Ginterseder, B. Spokoyny, N. D. Klein, K. E. Shulenberger, C. F. Perkinson, M. V. Kovalenko, and M. G. Bawendi, "Coherent single-photon emission from colloidal lead halide perovskite quantum dots," Science **363**, 1068–1072 (2019).
[53]M. J. Crane, L. M. Jacoby, T. A. Cohen, Y. Huang, C. K. Luscombe, and D. R. Gamelin, "Coherent spin precession and lifetime-limited spin

dephasing in $CsPbBr_3$ perovskite nanocrystals," Nano Lett. **20**, 8626–8633 (2020).
[54]L. M. Herz, "How lattice dynamics moderate the electronic properties of metal-halide perovskites," J. Phys. Chem. Lett. **9**, 6853–6863 (2018).
[55]T. R. Hopper, A. Gorodetsky, A. Jeong, F. Krieg, M. I. Bodnarchuk, M. Maimaris, M. Chaplain, T. J. Macdonald, X. Huang, R. Lovrincic, M. V. Kovalenko, and A. A. Bakulin, "Hot carrier dynamics in perovskite nanocrystal solids: Role of the cold carriers, nanoconfinement, and the surface," Nano Lett. **20**, 2271–2278 (2020).
[56]K. Miyata, D. Meggiolaro, M. T. Trinh, P. P. Joshi, E. Mosconi, S. C. Jones, F. De Angelis, and X.-Y. Zhu, "Large polarons in lead halide perovskites," Sci. Adv. **3**, e1701217 (2017).